Research Square

Preprints are preliminary reports that have not undergone peer review.
They should not be considered conclusive, used to inform clinical practice,
or referenced by the media as validated information.

Mitigation Technologies for Wellbore Blockage Caused by Coal Powder Ejection from Surface Wells in Mining-Disturbed Areas: A Case Study

Wei Qin
China University of Mining and Technology
Yong Deng
China University of Mining and Technology
Guozhong Hu
China University of Mining and Technology
Jialin Xu
China University of Mining and Technology
Wentao Ji
Huaibei Mining Industry Co., Ltd
Lu Che
Huaibei Mining Industry Co., Ltd
Haoran Duan
TB23020004A41LD@cumt.edu.cn

China University of Mining and Technology

Research Article

Keywords: Wellbore blockage, Surface well, Gas drainage, Coal powder ejection, Mining-disturbed areas

Posted Date: August 13th, 2026

DOI: https://doi.org/10.21203/rs.3.rs-10560065/v1

License: This work is licensed under a Creative Commons Attribution 4.0 International License.
Read Full License

Additional Declarations: No competing interests reported.

Mitigation Technologies for Wellbore Blockage Caused by Coal Powder Ejection from Surface Wells in Mining-Disturbed Areas: A Case Study

Wei Qin [1], Yong Deng [2], Guozhong Hu [2], Jialin Xu [1], Wentao Ji [3], Lu Che [3], Haoran Duan [2,*]

[1] State Key Laboratory for Fine Exploration and Intelligent Development of Coal Resources, China University of Mining and Technology, Xuzhou, Jiangsu, 221116, China

[2] School of Mines, China University of Mining and Technology, Xuzhou, Jiangsu, 221116, China

[3] Huaibei Mining Industry Co., Ltd., Huaibei, Anhui, 235047, China

Correspondence should be addressed to Haoran Duan; Email: TB23020004A41LD@cumt.edu.cn.

Abstract: Surface wells drilled in mining-disturbed areas are an effective means for pressure-relief gas drainage. In soft, outburst-prone coal seams, however, high-pressure gas can carry coal powder into the wellbore, causing severe plugging and a consequent decline in drainage efficiency. Intense mining disturbance, low coal strength, and high gas pressure were identified as the primary contributing factors. High-pressure gas flushing was applied to alleviate the blockage. Results show that flushing is most effective when the working face is positioned directly beneath the well, yielding an average peak gas flow rate of 30.9 m³/min and sustaining a rate above 10 m³/min for 57.5 days. A standpipe installed inside the slotted pipe was also tested, but coal powder continued to enter through the drain holes, rendering this approach ineffective. A third alternative—fitting a metal mesh filter around the slotted pipe—was subsequently proposed. Laboratory tests indicated that while the mesh effectively retained coal powder, it also reduced gas flow; a 1.0 mm mesh size was identified as optimal. In field applications, wells 1024-2 and 1024-3, equipped with the 1.0 mm mesh, achieved an average peak flow rate of 27.29 m³/min and maintained a flow above 10 m³/min for 45.5 days, confirming satisfactory performance in mitigating wellbore plugging.

Keywords: Wellbore blockage; Surface well; Gas drainage; Coal powder ejection; Mining-disturbed areas

1 Introduction

Coal seam gas, primarily composed of methane, poses a serious threat to mine safety but also represents a clean and efficient energy source(Huang et al. 2022; Zheng et al. 2024). One cubic meter of methane has a calorific value roughly equivalent to 1.25 kg standard coal or 1.13 kg gasoline(Jackson and Kershaw 1996). China holds abundant coalbed methane (CBM) resources, with estimated geological reserves of about 30.05×10^{12} m^3 within a depth of 2000 m and recoverable reserves of approximately 12.50×10^{12} m^3 (Zhang et al. 2018). In 2025, the country's CBM drainage reached 1.813×10^{10} m^3, accounting for 8% of the national natural gas output. Developing and utilizing this resource is essential for reducing gas-related accidents, diversifying the natural gas supply, and cutting greenhouse gas emissions(Karacan et al. 2011; Li et al. 2025a; Ma et al. 2021; Xiao and Chen 2022). At present, gas drainage remains the principal measure for both gas control and clean energy recovery. However, most gassy coal seams in China are characterized by soft coal, low permeability, low gas saturation, and high adsorption capacity(Hua et al. 2025). Consequently, gas production from surface fractured wells in undisturbed areas declines rapidly. By 2022, among more than 24,000 such wells drilled nationwide, 57% produced less than 600 m^3/d(Li et al. 2023).

Previous studies have shown that intense strata movement induced by coal mining not only relieves stress in adjacent seams and promotes gas desorption but also creates and extends interconnected fractures within the overburden(Khademian et al. 2022). These fractures provide extensive migration pathways and storage space for pressure-relieved gas, producing a significant “pressure relief and permeability enhancement” effect(Palchik 2003). Surface wells placed in mining-disturbed areas exploit this mechanism(Karacan 2015). Typically, a vertical well is drilled before mining, passing through several gassy coal seams and terminating near the coal seam roof. Once mining begins, the gob fractures connect with the well, allowing large-scale drainage of gas released from both the working seam and adjacent seams. Since these wells are drilled from the surface, they are relatively easy to construct and do not interfere

with underground coal extraction, making them popular across Chinese mining districts. Over the past decade of theoretical and field research, China has made significant progress in establishing principles for well layout(Ren et al. 2018), spacing(Hu and Sun 2014), and structural design(Sun et al. 2009, 2011). A key finding is that locating wells 20-70 m from the return airway benefits gas drainage, and placing them within 30 m of the return airway while moderately increasing hole diameter improves well stability. Three generations of well structures have been developed(Yuan et al. 2013), along with a flexible-joint protection device that effectively prevents well breakage(Cheng and Li 2022), thereby extending the effective service life of surface wells.

Currently, coal mining depth in China is increasing at a rate of 10-25 m/a. Deep gassy seams are characterized by high in-situ stress, high gas pressure, high gas content, and intense mining disturbance. This is especially true in the Huaibei and Huainan mining areas of eastern China, where nearly all mines are highly gassy or prone to coal-and-gas outbursts. In these areas, gas pressures typically range from 2 to 7 MPa and gas contents from 10 to 26 m^3/t; at depths of 800-1000 m, these values often reach or exceed the upper limits. During pressure-relief gas drainage via surface wells, the Huaibei and Huainan areas have commonly experienced coal powder ejection and wellbore blockage originating from adjacent strong-outburst seams. Coal powder accumulations exceeding 100 m in height have been observed, severely impairing gas drainage efficiency. A typical example is the Luling Coal Mine in the Huaibei District, where gas content reaches 15.8 m^3/t and gas pressure ranges from 2 to 5.7 MPa. At its 1022 working face, 22 surface wells experienced varying degrees of coal powder ejection and blockage, significantly reducing both peak drainage rates and effective drainage duration. Pre-mining fractured wells also encounter coal powder production, but without mining disturbance, the coal powder volume is lower, the release rate is slower, and the particle size is smaller. The underlying technical principles, drainage methods, and effective timing differ markedly from those of surface wells in mining-disturbed areas. Consequently, existing research on coal powder production mechanisms, accumulation patterns, and mitigation methods for pre-mining fractured wells(Cui et al. 2016; Du et al. 2018; Han et al. 2016; Li et al. 2025b; Liu et al. 2025; Meng 2024; Mu et al. 2020; Ren et al. 2025; Wei et al. 2017, 2022; Xu et al. 2025; Zhang et al. 2020, 2025; Zhao et al. 2016) cannot be directly applied to mining-disturbed wells.

To mitigate the problem of wellbore blockage induced by coal powder ejection, the Luling Coal Mine tested several countermeasures: high-pressure gas flushing, installing a standpipe inside the slotted pipe, and adding a metal mesh filter outside the slotted pipe. Positive results were obtained, offering a reference for similar conditions involving soft, strong-outburst seams. This paper first describes the phenomenon of coal powder ejection and its impact on gas drainage at the III1022 working face of the Luling Coal Mine, identifying the main causes of blockage. It then discusses each mitigation method and its effectiveness, selects the most promising approach, and presents a satisfactory outcome for pressure-relief gas drainage using surface wells in a mining-disturbed area.

2 Coal powder ejection and wellbore blockage in surface gas drainage wells in mining-disturbed areas: Phenomena and hazards

2.1 Engineering background

The Luling Coal Mine, located in the Huaibei mining area, is a typical high-gas outburst mine. Outburst risks are primarily mitigated through protective seam extraction. The principle is as follows: the lower No. 10 coal seam, which has a relatively lower outburst potential, is extracted first. The resulting mining-induced stress relief and permeability enhancement in the overburden, along with gas pressure relief and desorption in adjacent seams, enable gas drainage from the overlying Nos. 7, 8, and 9 coal seams via surface wells. This approach reduces gas emissions into the No. 10 working face while also lowering the gas content and pressure in the overlying seams, thereby achieving regional outburst elimination and creating favorable conditions for future extraction of the Nos. 7, 8, and 9 coal seams.

The 1022 working face is the first panel of the third level in the mine's second mining district (Fig. 1). It extracts

the No. 10 coal seam, which ranges from 1.3 m to 3.2 m in thickness (average 2.67 m). The panel is situated at elevations between -654.9 m and -742.5 m, with an average strike length of 1406.6 m and a face length of 175 m. The seam thickness is relatively stable, showing no significant variation. The dip angle ranges from 15° to 28°, with an average of 17°. The industrial reserve is 891,000 t, and the estimated recoverable amount is 846,500 t. At the 1022 working face, the measured maximum original gas pressure in the No. 10 coal seam is 2.6 MPa, and the maximum original gas content is 13.7 m^3/t—both exceeding the regulatory critical values for outburst prevention (0.75 MPa and 8 m^3/t). The 1024 working face lies to the north of the 1022 face and also extracts the No. 10 coal seam. Here, seam thickness ranges from 1.94 m to 2.93 m (average 2.54 m). The panel elevation is -724.5 m to -815.5 m, with an average strike length of 1423.3 m and a face length of 165 m. The dip angle varies from 3° to 41°, averaging 18°. The industrial reserve is 790,200 t, and the estimated recoverable amount is 750,700 t. At the 1024 working face, the measured maximum original gas pressure in the No. 10 coal seam is 1.74 MPa, and the maximum original gas content is 11.20 m^3/t—again above the regulatory thresholds. The overlying Nos. 7, 8, and 9 coal seams above both working faces are extremely soft, with Protodyakonov's coefficients of approximately 0.1-0.3. Their gas pressures reach 4.43-6.47 MPa, and gas contents are 22-25 m^3/t, making them typical soft, strong-outburst coal seams.

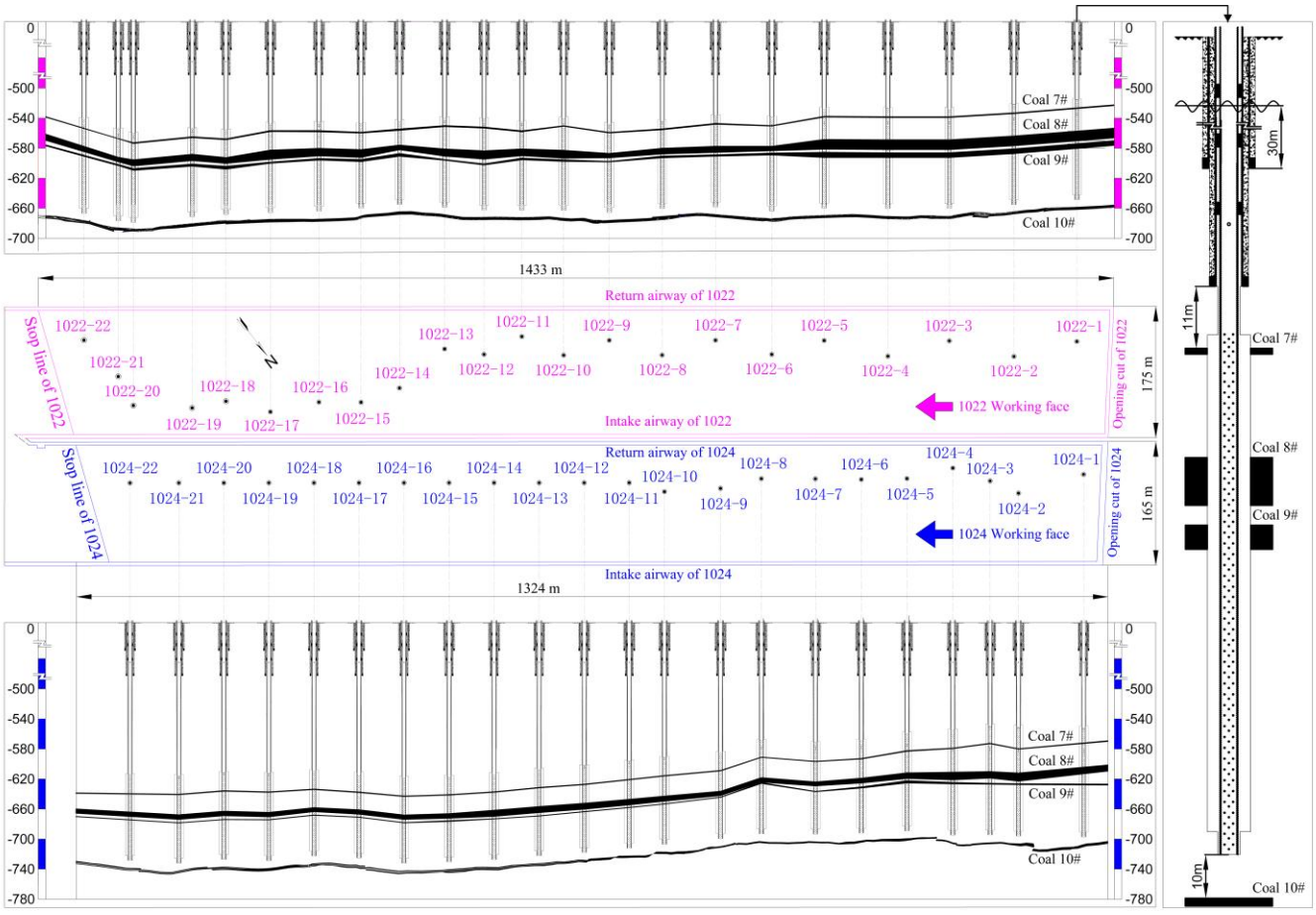


Fig. 1 Layout of surface wells in the mining-disturbed area of the 1022 and 1024 working faces in the Luling Coal Mine.

To reduce gas emission during extraction of the No. 10 coal seam while simultaneously lowering the gas pressure and content in the overlying Nos. 7, 8, and 9 coal seams, surface wells for pressure-relief gas drainage were deployed in both the 1022 and 1024 working faces. Twenty-two surface wells were drilled for each face, with their layout shown in Fig. 1. Wells 1022-1 through 1022-13 and 1022-22 are located on the return airway side, spaced 50-80 m apart and positioned 35-60 m from the return airway. Because the ground on the return-airway side was wet and unsuitable for construction, wells 1022-14 through 1022-21 were placed on the intake airway side, with a spacing of

50-80 m and a distance of 45-75 m from the intake airway. All wells at the 1024 face (1024-1 through 1024-22) are located on the return airway side, spaced 50-75 m apart and 40-60 m from the return airway.

Among the 22 surface wells drilled at the 1022 working face, Nos. 1022-1 through 1022-5 are classified as Type B. With the exception of Nos. 1022-18 and 1022-21, which are Type D, the remaining wells are Type C. At the 1024 working face, all 22 wells are Type C, except for Nos. 1024-3 and 1024-7, which are Type D. Detailed design parameters for each well type are summarized in Table 1. The structural design follows a three-section configuration. The first section extends to a depth of 30 m below the base of the loose strata. The second section ends 11 m above the roof of the No. 7 coal seam. The third section terminates 10 m above the roof of the No. 10 coal seam. Logging data from the surface wells at the 1022 and 1024 working faces indicate that the No. 7 coal seam has an average thickness of 1.7 m and lies 110-130 m above the No. 10 coal seam. The No. 8 coal seam averages 10.1 m in thickness and is located 80-90 m above the No. 10 coal seam. The No. 9 coal seam averages 3.6 m and lies 70-85 m above the No. 10 coal seam. To enhance gas drainage performance, under-reaming was applied in the third section, starting from 15 m above the roof of the No. 10 coal seam. The under-reamed diameter is 420 mm for Type B and Type C wells and 550 mm for Type D wells. The under-reamed interval covers the No. 7, No. 8, and No. 9 coal seams.

Table 1. Detailed design parameters of various types of surface wells.

Well type	First spud diameter/mm	First casing/mm	Second spud diameter/mm	Second casing/mm	Third spud diameter/mm	Third casing/mm	Undercutting diameter/mm	Undercutting section
B	508	406	375	273	216	177.8	420	15 m to 135 m above the roof of No. 10
C	630	480	444.5	339.7	269.9	219.1	420	15 m to 110 m above the roof of No. 10
D	880	710	660	508	444.5	339.7	550	15 m to 120 m above the roof of No. 10

2.2 Coal powder ejection and hole blockage: observations and impact on gas drainage performance

During extraction at the 1022 working face, field measurements were taken for both coal powder accumulation and gas drainage flow rates from the surface wells. Every well showed signs of coal powder ejection and blockage. Among them, wells 1022-6 through 1022-9 received no remedial interventions, and their measured coal powder accumulation heights and gas drainage flow rates are presented in Fig. 2. In the figure, negative distances on the horizontal axis indicate that the working face has not yet passed the well, while positive values mean the working face has moved beyond it. The measurements show no coal powder accumulation when the working face is 200 m away from the well. As the face approaches within 0-30 m, the coal powder accumulation rate rises sharply, peaking when the face lies directly beneath the well. At that moment, the peak accumulation rates for wells 1022-6, 1022-7, 1022-8, and 1022-9 reach 5.8 m/d, 13.7 m/d, 1.30 m/d, and 7.00 m/d, respectively. After the face passes the well by 30 m, the accumulation rate declines.

Under normal operating conditions for a Type C well, the peak gas drainage flow rate typically exceeds 25 m^3/min, and a high flow rate (above 10 m^3/min) can be sustained for about 50 days. However, in wells 1022-6 through 1022-9, the accumulated coal powder reached heights of 89-101 m, extending above the roof of the No. 8 coal seam. This buildup severely impaired gas drainage performance. The peak flow rates for wells 1022-6, 1022-7, 1022-8, and 1022-9 were 15.6 m^3/min, 11.4 m^3/min, 17.1 m^3/min, and 9.8 m^3/min, respectively, averaging 13.5 m^3/min. The number of days during which the gas flow rate remained above 10 m^3/min was 22, 17, 18, and 0, respectively, giving an average of only 14.3 days. After the working face passes the well by 50-60 m, the net gas drainage flow rate steadily declines. These observations indicate that coal powder accumulating inside the well casing seriously obstructs gas flow. Furthermore, the blockage prevents mining-induced fractures from effectively

connecting with the surface well, and water inside the well cannot drain into the goaf in time. As a result, pressure-relieved gas in the goaf is not extracted efficiently, leading to increased gas emissions at the 1022 working face.

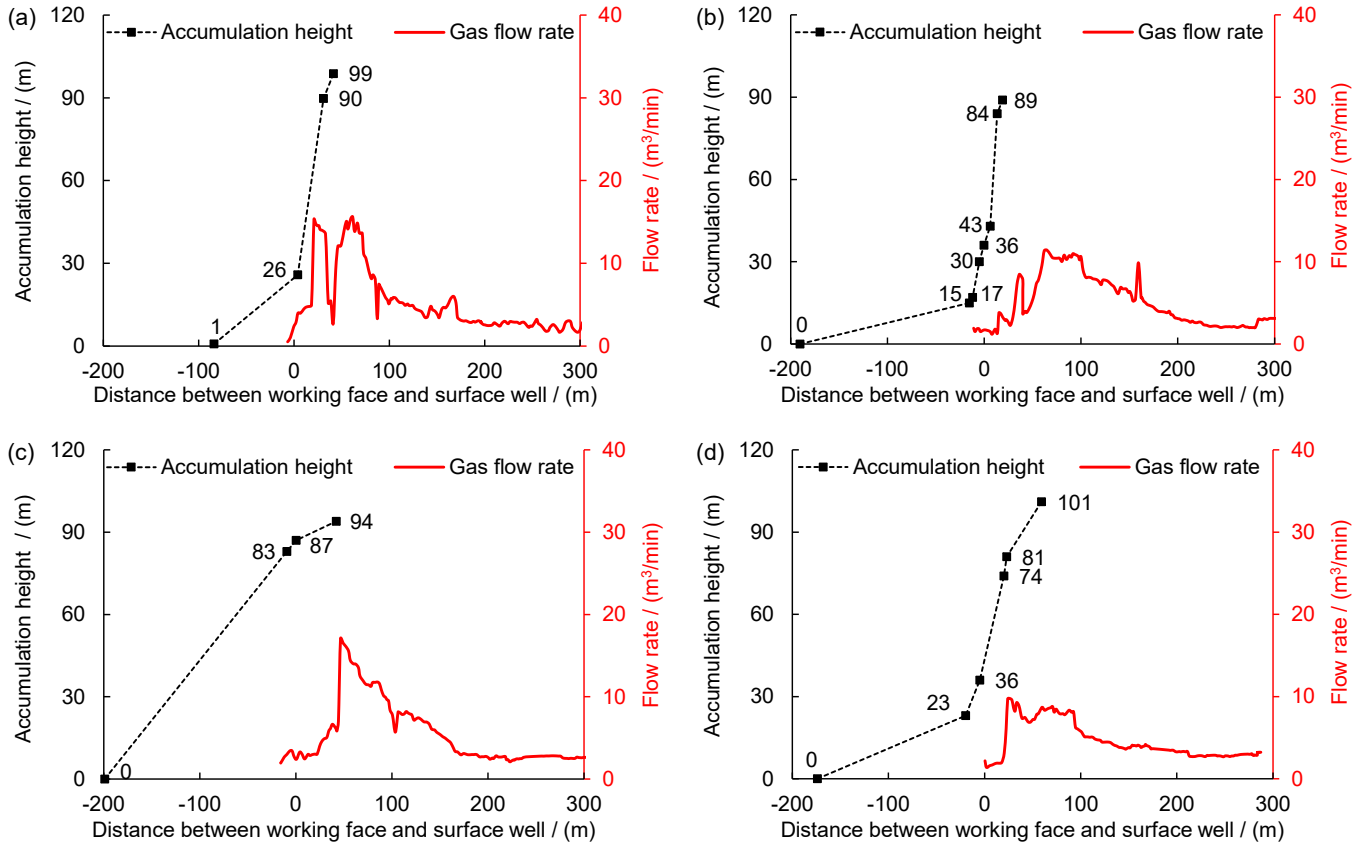


Fig. 2 Test results of coal powder accumulation height and gas drainage flow rate for wells. (a) well 1022-6; (b) well 1022-7; (c) well 1022-8; (d) well 1022-9.

2.3 Main causes of coal powder ejection and hole blockage

The coal powder accumulation curves in Fig. 2 reveal that when the surface well lies more than 200 m ahead of the working face, no coal powder accumulates inside the casing. This observation indicates that the overlying adjacent coal seams remain unaffected by mining activity at this stage. Their permeability stays low, gas release is slow, and no gas ejection occurs. Only a minor amount of fine coal particles enters the well casing, as illustrated in Fig. 3a. When the well is about 30 m ahead of the working face, coal powder accumulation begins to intensify. At this stage, the face is close enough to induce stress concentration in the adjacent seams. The soft coal, subjected to vertical stress concentration, tends to pulverize, further increasing the rate of coal powder ejection (Fig. 3b). When the well lies within 0-30 m of the working face, the accumulated height rises sharply. By this point, the mining-induced pressure relief zone has reached the overlying adjacent seams. These seams expand as pressure is released, and their permeability increases rapidly. Gas in the coal seam quickly shifts from the adsorbed state to the free state and jets into the surface well, carrying large amounts of coal powder into the casing (Fig. 3c). In summary, two key factors account for coal powder ejection and blockage in the surface wells at the Luling Mine's 1022 working face. First, the adjacent seams are extremely soft, making them prone to pulverization under advanced stress concentration. Second, these seams have high gas pressure and high gas content. Once pressure is relieved, gas desorbs rapidly, providing a strong pneumatic driving force for coal powder ejection.

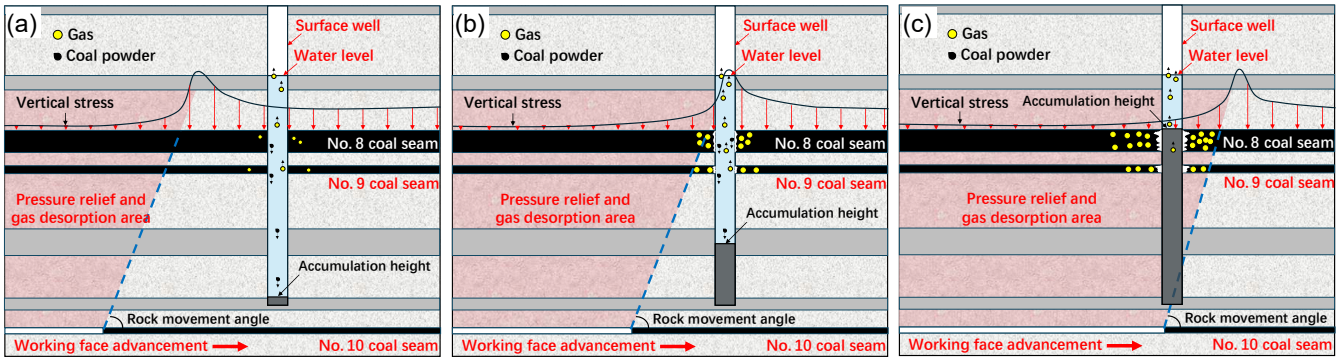


Fig. 3 Mechanism of coal powder ejection from surface wells in the mining-disturbed area during working face advancement. (a) surface well lies more than 200 m ahead of the working face; (b) well is about 30 m ahead of the working face; (c) well lies within 0-30 m of the working face.

3 Technologies for preventing coal powder hole blockage in surface wells

To address the problem of coal powder ejection and hole blockage in surface wells, the Luling Coal Mine tested various countermeasures in subsequent wells. The goal was to reduce the height of coal powder accumulation, maintain well openness, and thereby improve gas drainage performance. The following sections describe the implementation and field effectiveness of each technique, offering practical references for pressure-relief gas drainage under similar conditions.

3.1 High-pressure gas flushing for coal debris removal

When coal powder accumulation was first observed, the initial remedial approach involved injecting high-pressure gas into the well bottom through a drill pipe, using the high-velocity airflow to blow coal powder and water out of the well. This gas-flushing method was applied to wells 1022-10 through 1022-17, with an injection pressure of 7.0-8.5 MPa and a gas flow rate of 60-65 m^3/min. The timing of flushing varied among these eight wells. For wells 1022-10, 1022-11, and 1022-12, flushing was carried out when the working face was still more than 100 m away from the well. Well 1022-13 was flushed after the face had advanced 27 m past the well. Wells 1022-14 through 1022-17 were flushed when the face was directly beneath the well. After flushing, continuous monitoring was performed on both coal powder accumulation height and gas drainage flow rate. The results for wells 1022-10, 1022-11, 1022-12, and 1022-13 are shown in Fig. 4, where the blue points indicate coal powder accumulation height after flushing. In wells 1022-10, 1022-11, and 1022-12 (flushed when the face was >100 m away), the coal powder accumulation dropped to zero, achieving the desired immediate effect. However, as mining progressed, coal powder re-accumulated. By the time the face reached these wells, the accumulated heights had risen again to 65 m, 23 m, and 67 m, respectively. This indicates that early flushing temporarily removes coal powder but does not prevent subsequent coal powder ejection. Regarding gas drainage performance, the peak flow rates for wells 1022-10, 1022-11, and 1022-12 were 23.6 m^3/min, 15.0 m^3/min, and 20.0 m^3/min, respectively, averaging 19.5 m^3/min—an improvement of 44% over untreated wells. The number of days during which gas flow exceeded 10 m^3/min for wells 1022-9 (untreated reference), 1022-11, and 1022-12 was 41, 33, and 30 days, respectively, averaging 34.7 days—a 143% increase compared with untreated wells. For well 1022-13, flushed 27 m after the face had passed, the coal powder height decreased from 85 m to 10 m, but the problem was not fully resolved. A possible explanation is that after the face advances beyond the well by 27 m, mining-induced fractures in the goaf may connect with the well, allowing some of the injected high-pressure gas to escape into the goaf. This reduces the ability of the gas jet to carry coal powder back to the surface. Nevertheless, after flushing, well 1022-13 achieved a peak flow rate of 24.5 m^3/min and sustained a flow above 10 m^3/min for 64 days—significantly better than wells flushed too early.

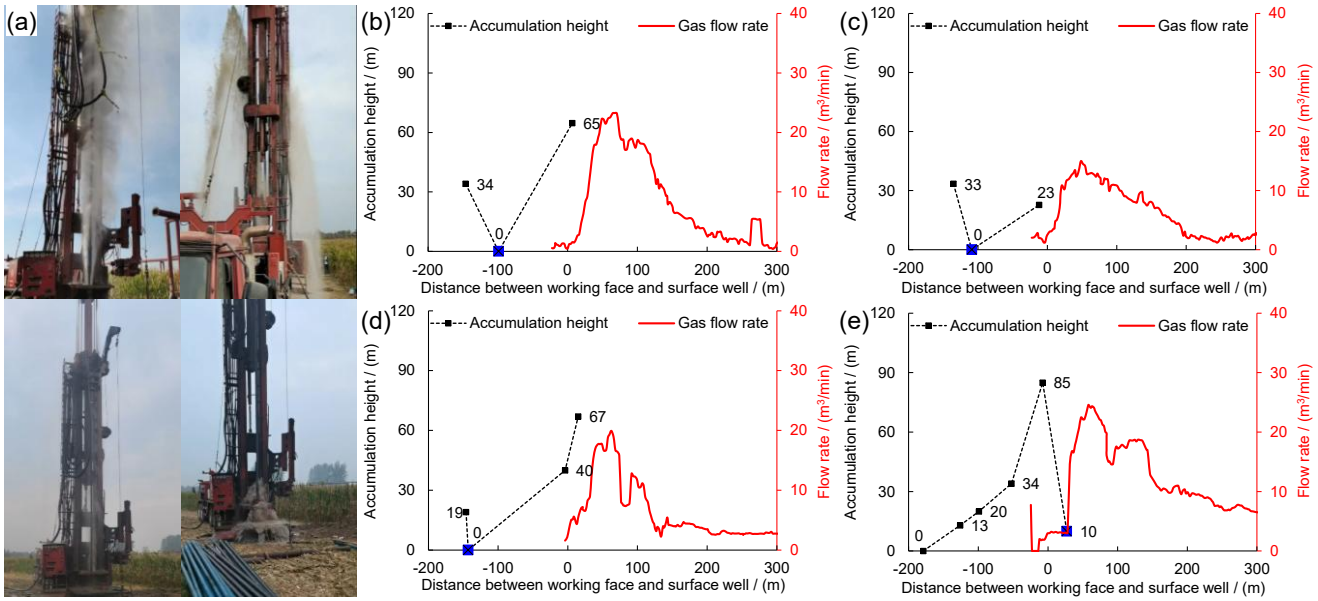


Fig. 4 Test results of coal powder accumulation height and gas drainage flow rate for wells. (a) field photographs; (b) well 1022-10; (c) well 1022-11; (d) well 1022-12; (e) well 1022-13.

Wells 1022-14, 1022-15, 1022-16, and 1022-17 were flushed with high-pressure gas precisely when the working face was positioned directly beneath the well. The test results are presented in Fig. 5, where the blue points indicate the coal powder height after flushing. Before the working face reached the well location, coal powder accumulation height in these four wells had already reached 69 m, 72 m, 70 m, and 92 m, respectively. After flushing, the powder height dropped to zero in all four wells, effectively resolving the blockage problem. Regarding gas drainage performance, the peak flow rates for wells 1022-14, 1022-15, 1022-16, and 1022-17 reached 31.1 m^3/min, 33.5 m^3/min, 29.4 m^3/min, and 29.6 m^3/min, respectively. The number of days during which the gas flow exceeded 10 m^3/min was 57, 62, 63, and 48 days, respectively. Averaging across these four wells, the peak flow rate was 30.9 m^3/min—129% higher than that of untreated wells. The average duration with a flow above 10 m^3/min was 57.5 days, representing a 302% improvement compared with untreated wells.

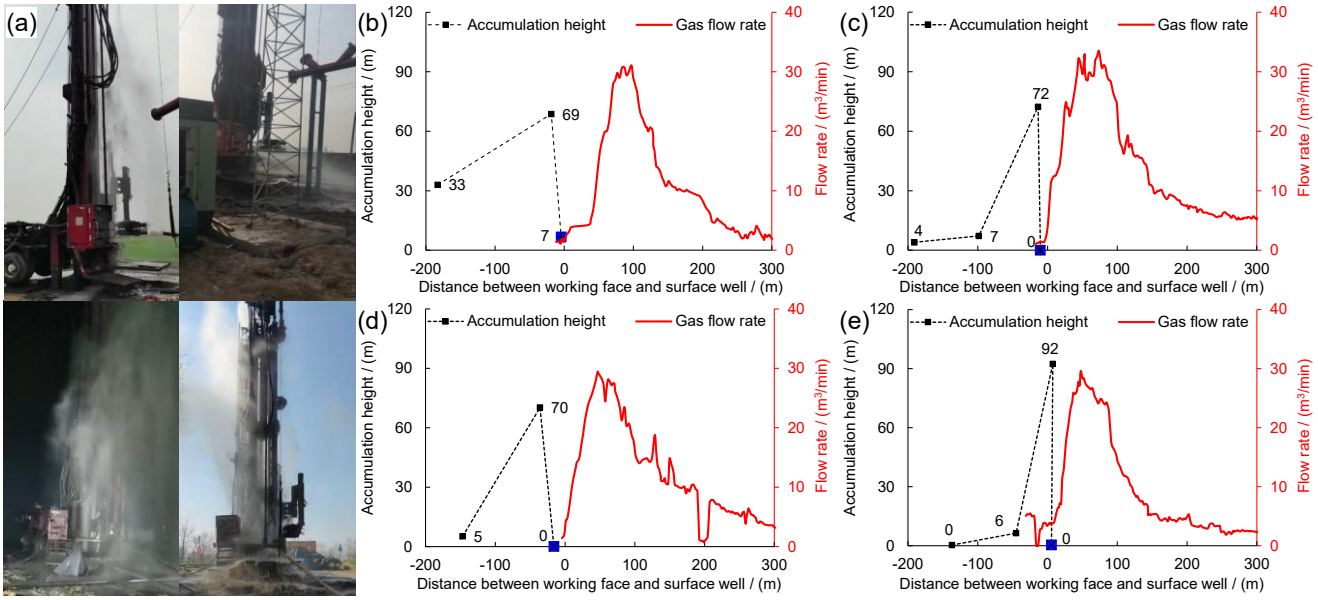


Fig. 5 Test results of coal powder accumulation height and gas drainage flow rate for wells. (a) field photographs; (b) well 1022-14; (c) well 1022-15; (d) well 1022-16; (e) well 1022-17.

3.2 Installation of a standpipe inside the slotted pipe

Field observations indicated that coal powder accumulation appears unavoidable as the working face approaches the surface well. To mitigate its impact on gas drainage performance, maintaining connectivity between the well and the goaf is essential. Accordingly, this study proposes installing a standpipe inside the slotted pipe. The standpipe is a solid tube with a diameter of 127 mm, considerably smaller than the slotted pipe diameter of 219 mm. To prevent coal powder from entering the standpipe, its upper end should be positioned above the maximum expected coal powder accumulation height (101 m). The layout scheme is shown in Fig. 6a. To allow water inside the standpipe to drain downward into the goaf and avoid water blocking the pipe, two drain holes were placed at the lower end of the standpipe in well 1022-19. In wells 1022-20 and 1022-21, two drain holes were arranged every 1 m along the entire pipe wall. Field measurements of coal powder accumulation height and gas drainage flow rate were then conducted for these three wells; the results are shown in Fig. 6b,c,d. Despite the standpipe, well 1022-19 still experienced some coal powder accumulation, but the height remained small, peaking at 15 m. Its peak gas drainage flow rate reached 30.8 m^3/min, and it sustained a flow above 10 m^3/min for 38 days. In contrast, wells 1022-20 and 1022-21 suffered severe coal powder accumulation, with heights reaching 86 m and 69 m, respectively. Although high-pressure gas flushing subsequently reduced these heights to 16 m and 18 m (blue points in Fig. 6c,d, gas drainage was significantly affected. Their peak flow rates were 18.6 m^3/min and 23.8 m^3/min, averaging 21.2 m^3/min. The durations with flow above 10 m^3/min were 39 and 43 days, averaging 41 days. Compared with wells 1022-14 through 1022-17 (flushed when the face was directly beneath the well), the average peak flow rate of wells 1022-20 and 1022-21 dropped by 31.4%, and the average high-flow duration fell by 28.7%. Their performance was also inferior to that of well 1022-13, which was flushed after the face had advanced 27 m past the well. The main reason for coal powder accumulation in wells 1022-19, 1022-20, and 1022-21 is that coal powder entered the standpipe through the drain holes. Well 1022-19 had only two drain holes, so the accumulation height remained small. Wells 1022-20 and 1022-21, however, had 260 drain holes, leading to much larger accumulations that eventually required high-pressure gas flushing to improve gas drainage.

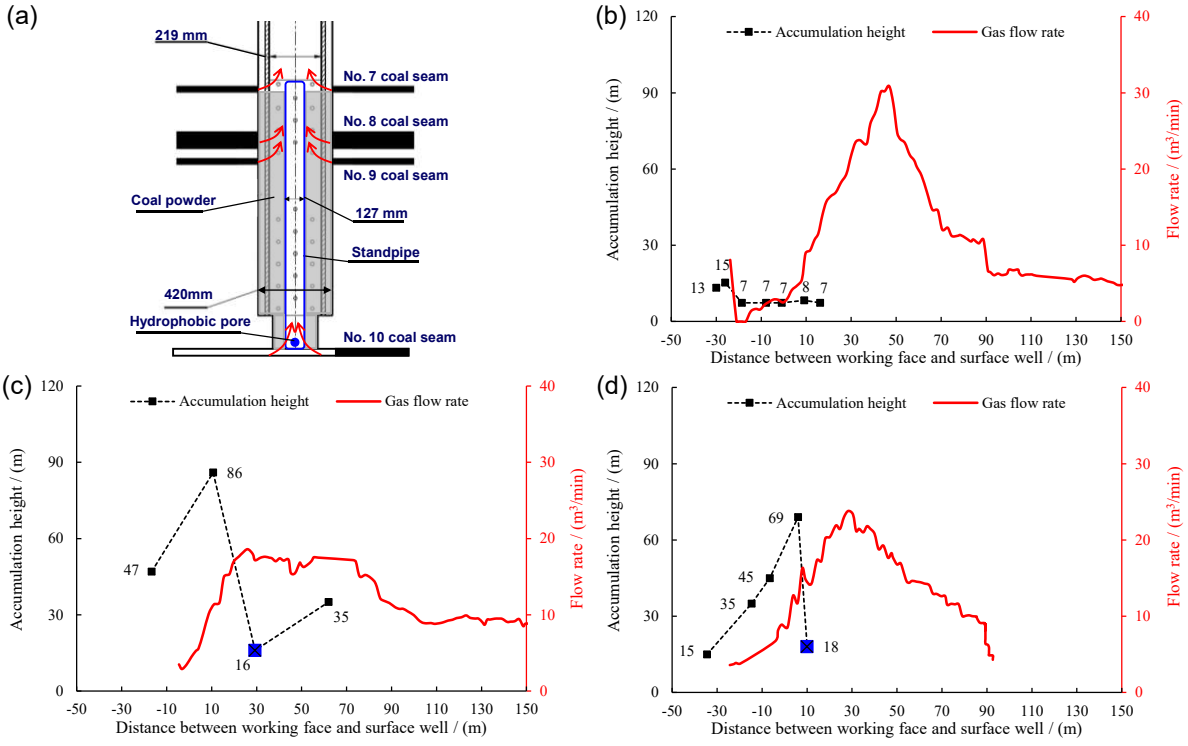


Fig. 6 Test results of coal powder accumulation height and gas drainage flow rate for wells. (a) schematic diagram of standpipe installation; (b) well 1022-19; (c) well 1022-20; (d) well 1022-21.

3.3 Installation of a metal mesh filter

Since the standpipe did not effectively prevent coal powder accumulation and also added an extra casing string—increasing both construction cost and workload—this study proposes an alternative method: installing a metal mesh filter outside the slotted pipe to keep coal powder from entering. However, this approach raises several questions. What mesh size should be selected? Can the installed filter effectively block powder ingress? Will powder accumulating outside the filter impede gas flow into the pipe and thus reduce gas drainage performance? To address these questions, a laboratory test device was developed to simulate powder accumulation with metal mesh filters. A series of experiments were carried out, and the results provided guidance for gas drainage engineering using surface wells in the mining-disturbed area of the 1024 working face.

3.3.1 Coal powder particle size analysis

To determine the particle size distribution for the laboratory tests, coal powder was collected from well 1024-1 (Fig. 7a). The retrieved powder was wet; to facilitate sieving, it was first dried. A standard sieve set with mesh openings of 0-0.32 mm, 0.32-0.63 mm, 0.63-1.25 mm, 1.25-2.5 mm, 2.5-5 mm, and 5-10 mm was used (Fig. 7b). Sieving was carried out in 4 separate batches, each starting with 900 g of raw coal powder. The sieved fractions are shown in Fig. 7c,d,e,f. The average mass percentages for each size fraction were as follows: 0-0.32 mm: 4%; 0.32-0.63 mm: 11%; 0.63-1.25 mm: 13%; 1.25-2.5 mm: 43%; 2.5-5 mm: 25%; and 5-10 mm: 3% (Fig. 7g). These proportions were used to prepare artificial coal powder for the subsequent metal mesh filter tests.

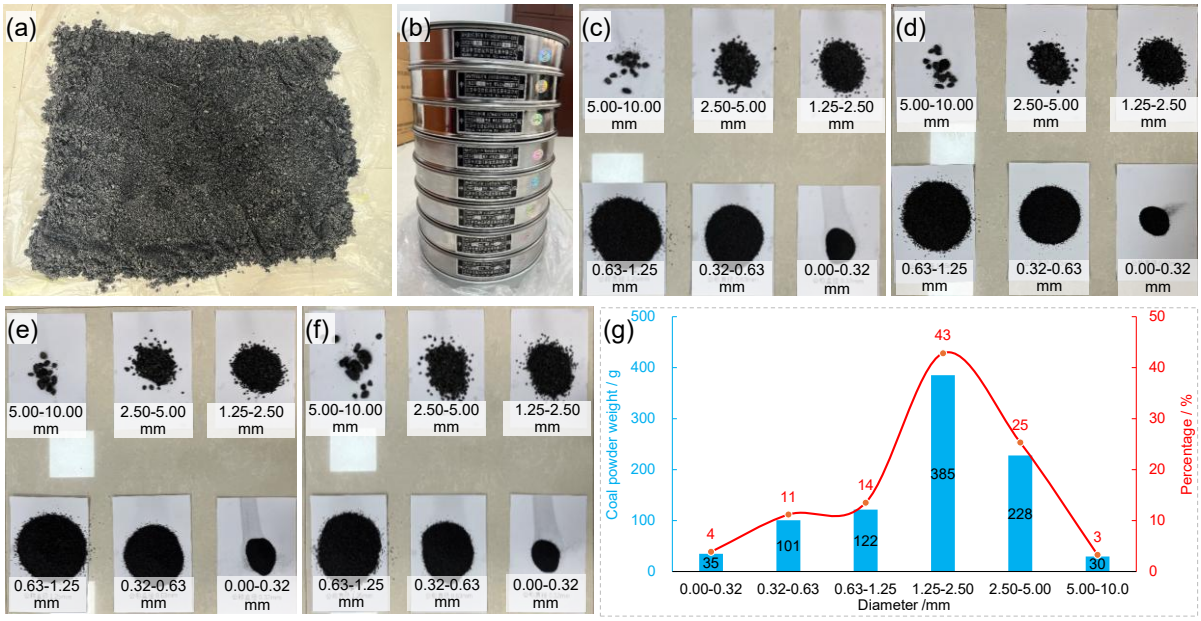


Fig. 7 Coal powder sieving procedure and particle size gradation scheme of experimental coal powder. (a) coal powder; (b) standard sieves of different mesh sizes; (c) coal powder sample 1; (d) coal powder sample 2; (e) coal powder sample 3; (f) coal powder sample 4; (g) particle size distribution of coal powder.

3.3.2 Experimental setup

The experimental device for evaluating coal powder accumulation control using a metal mesh filter consists of the following components: an outer casing, an inner slotted pipe, a grouting pump, a grouting pipe, a top cover plate, a sealing flange, a one-way valve, a control panel, a discharge line, a gas-liquid separator, a gas flowmeter, a gas outlet pipe, two water drain pipes, an air compressor, a gas injection pipe, a device base, three pressure sensors (No. 1, No. 2, and No. 3), and four valves (No. 1, No. 2, No. 3 and No. 4). The structural design and physical appearance

of the device are shown in Fig. 8.

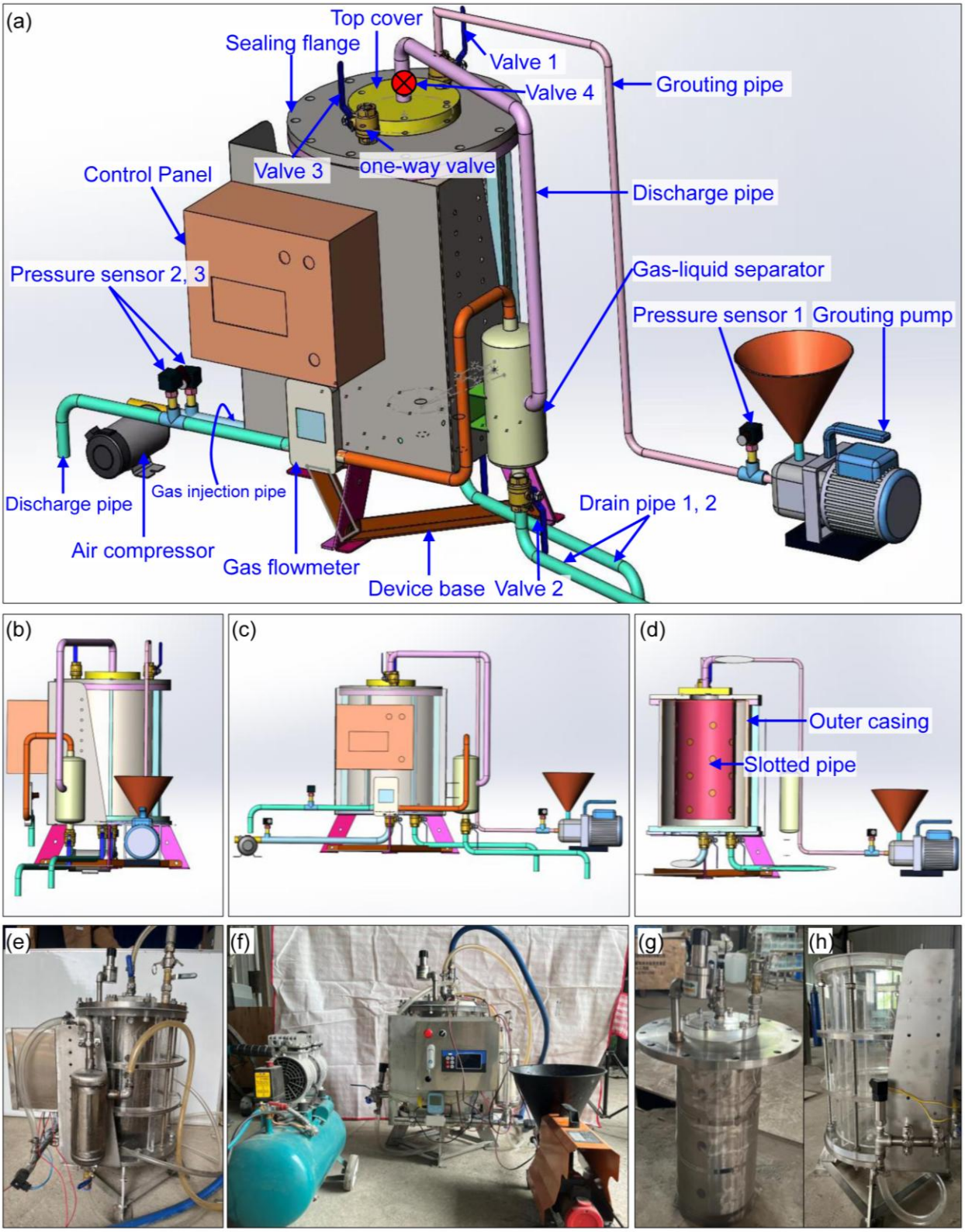


Fig. 8. Schematic diagram and photograph of the experimental setup for suppressing coal powder accumulation using a metal mesh. (a) Composition diagram of the device; (b) design drawing - side view; (c) Design drawing - front view; (d) Perspective drawing; (e) Physical - side view; (f) Physical drawing - front view; (g) outer casing; (h) inner slotted pipe.

The outer casing, which simulates a surface well, is made of transparent acrylic tubing. It was fabricated based on the diameter of the third section of a Type C well (269.9 mm) and has a height of 0.6 m. The inner slotted pipe is made of stainless steel, with its dimensions following the slotted pipe design of a Type C well (219 mm in diameter). It has a height of 0.5 m, with perforation holes of 24 mm in diameter spaced at 60 mm intervals. Four perforations are evenly distributed around the circumference at 90° intervals. Pressure sensors monitor the grouting pressure, gas inlet pressure, and gas outlet pressure, while a gas flowmeter measures the flow rate in the gas discharge line.

3.3.3 Experimental procedure

A coal-water mixture was prepared based on the particle size distribution results shown in Fig. 7g, using a water-to-cement ratio of 1:1. The preparation process is illustrated in Fig. 9a,b. A metal mesh filter was wrapped around the outside of the slotted pipe (Fig. 9c), ensuring complete coverage of all perforations. The mesh had square openings with side lengths of 0.5 mm, 1.0 mm, and 2.0 mm. The slotted pipe with the attached mesh was then inserted into the outer casing, and the sealing flange was tightened with bolts (Fig. 9d) to ensure a good seal. Valves 1, 2, 3, and 4 were opened, and the grouting pump was started. The coal-water mixture was pumped through the grouting line into the annular space between the outer casing and the slotted pipe (Fig. 9e), simulating the coal powder ejection process. After disassembling the test device, the filtering effectiveness of the mesh was examined (Fig. 9f,g).

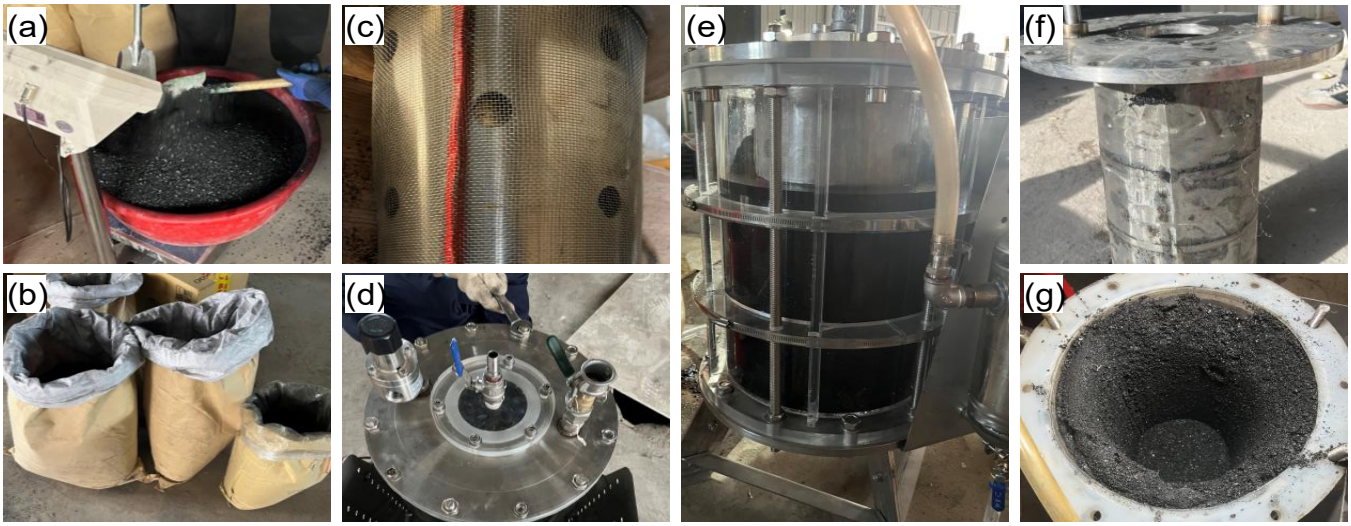


Fig. 9. Experimental procedure for suppressing coal powder accumulation using a metal mesh. (a) coal powder preparation; (b) coal powder; (c) metal filter mesh; (d) sealing flange; (e) coal powder ejection simulation apparatus; (f) slotted pipe; (g) filtration of coal powder using a mesh.

A grouting-first, gas-injection-later sequence was adopted. The opening pressure of the one-way valve was set at 0.5 MPa. When the internal pressure reached this value, the valve opened, and a constant grouting pressure of 0.5 MPa was maintained for five minutes. To identify a suitable metal mesh size, tests were performed with mesh openings of 0.5 mm, 1.0 mm, and 2.0 mm. To investigate the effect of grouting pressure, additional tests were conducted using a 1.0 mm mesh at grouting pressures of 0.75 MPa and 1.00MPa. Furthermore, to assess how the metal mesh affects gas flow capacity, a gas injection test was carried out after removing water from the device. Valves 1, 2, and 3 were closed, valve 4 was opened, and the air compressor was started. Gas pressure was raised stepwise using a pressure relief valve, and the gas flow rate in the discharge pipe was recorded at each pressure level. The test ended when the gas pressure reached 0.2 MPa. After the gas test, the inner slotted pipe was disassembled. The mass and height of coal powder that had entered the pipe were measured. The mesh was then replaced with another specification, and the entire procedure was repeated.

3.3.4 Experimental results

Valves 1, 2, 3, and 4 were closed, and the air compressor and gas injection valve were opened to raise the internal pressure to 1 MPa. The inlet valve was then closed, and a leak-tightness test was performed. The results are shown in Fig. 10a. The internal pressure did not drop noticeably within one hour, indicating good sealing performance. The grouting pressure evolution is shown in Fig. 10b. With a smaller mesh opening, fine coal particles quickly clogged the mesh, causing the grouting pressure to rise rapidly. For the 1.0 mm mesh, increasing the grouting flow rate also led to a quick pressure rise to the set levels (0.75 MPa and 1.0 MPa).

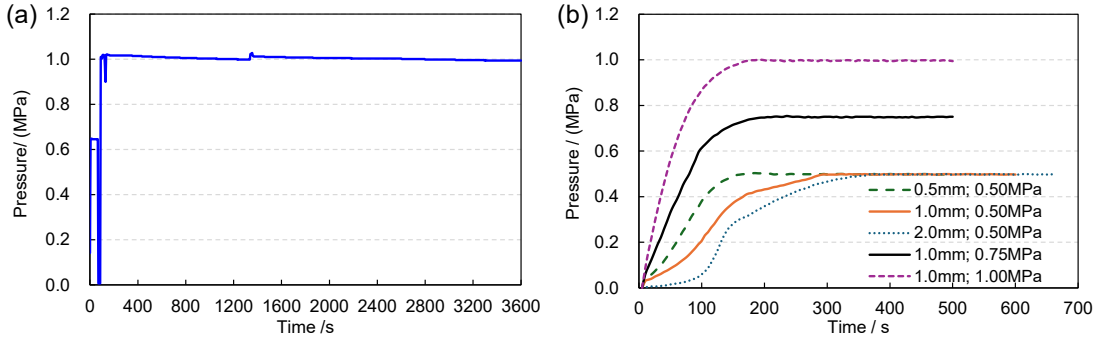


Fig. 10. Air tightness test results and grouting pressure variation curve of the experimental apparatus. (a) air tightness test result; (b) grouting pressure variation curve.

To evaluate how the metal mesh affects the gas drainage capacity of the slotted pipe, a gas injection test was conducted after each grouting experiment. A control test was also performed without grouting and without any mesh installed. The resulting coal powder accumulation inside the slotted pipe—both in weight and in height—is shown in Fig. 11a for different grouting conditions. The results confirm that installing the metal mesh effectively blocks coal powder from entering the slotted pipe. At a grouting pressure of 0.5 MPa, increasing the mesh opening from 0.5 mm to 2.0 mm raised the accumulated powder weight from 0.31 kg to 3.15 kg and the accumulation height from 0.82 cm to 7.9 cm—an increase of about ten times. Raising the grouting pressure also led to more powder entering the pipe. For the 1.0 mm mesh, increasing the grouting pressure from 0.5 MPa to 1.00 MPa caused the accumulated powder weight to rise from 0.31 kg to 1.72 kg and the accumulation height from 0.82 cm to 4.56 cm, roughly a 5.5-fold increase.

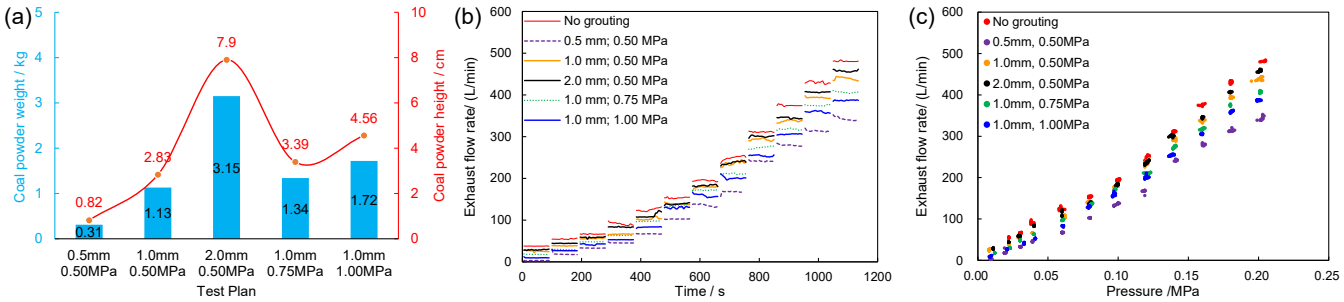


Fig. 11. Coal powder accumulation characteristics and variation curves of gas flow rate under different gas injection pressures. (a) variation curves of coal powder accumulation weight and height; (b) variation curve of gas flow rate with time; (c) variation curve of gas flow rate with pressure.

The gas flow rate in the exhaust line under different gas injection pressures is shown in Fig. 11b,c, with detailed test data listed in Table 2. As the injection pressure increases, the gas flow rate through the exhaust line rises accordingly. Grouting reduces the gas flow capacity of the slotted pipe because coal powder clogs the mesh openings.

This reduction is more pronounced at lower gas injection pressures. For a 0.5 mm mesh and a grouting pressure of 0.50 MPa, the gas flow capacity dropped by 22% to 92% compared with the un-grouted, no-mesh condition. With a 1.0 mm mesh under the same grouting pressure (0.50 MPa), the reduction ranged from 5% to 31%. For a 2.0 mm mesh at 0.50 MPa grouting pressure, the reduction was 3% to 24%. At a grouting pressure of 0.75 MPa with the 1.0 mm mesh, the reduction was 12% to 52%, and at 1.00 MPa grouting pressure with the same mesh, the reduction increased to 15%-75%. Overall, while the 2.0 mm mesh had the least impact on gas flow capacity, it allowed a large amount of coal powder to enter the slotted pipe, failing to fundamentally solve the blockage problem. The 0.5 mm mesh effectively blocked powder ingress but significantly reduced gas flow capacity. Considering both powder control and gas drainage performance, the 1.0 mm mesh is the recommended choice.

Table 2. Gas flow rate test data of the experimental apparatus exhaust pipe under different gas injection pressures.

Gas injection pressure/MPa	Exhaust flow rate under different grouting schemes (L/min)					
	No grouting	Mesh: 0.5 mm, Grouting: 0.50 MPa	Mesh: 1.0 mm, Grouting: 0.50 MPa	Mesh: 2.0 mm, Grouting: 0.50 MPa	Mesh: 1.0 mm, Grouting: 0.75 MPa	Mesh: 1.0 mm, Grouting: 1.00 MPa
0.01	37.7	3.1	25.7	28.6	18.0	9.5
0.02	54.8	18.7	38.3	44.1	29.6	26.6
0.03	66.6	33.0	55.9	58.4	48.0	41.7
0.04	91.3	45.6	66.3	83.2	63.3	52.8
0.06	125.1	67.2	103.1	110.8	97.3	83.0
0.08	153.5	102.6	138.9	138.4	134.9	129.8
0.10	194.8	135.7	178.7	182.7	171.8	158.7
0.12	249.2	167.6	235.7	237.6	211.0	201.2
0.14	311.5	241.6	293.0	300.8	274.0	254.2
0.16	375.0	279.7	337.3	345.0	317.8	305.9
0.18	430.3	313.8	393.6	406.9	374.9	359.5
2.00	480.9	342.8	439.1	457.7	406.5	387.1

3.3.5 Field application

During extraction of the 1024 working face, wells 1024-2 and 1024-3 were fitted with a 1.0 mm metal mesh covering the entire slotted pipe (Fig. 12a). Subsequent gas drainage monitoring and coal powder observations (Fig. 12b,c) showed that the mesh effectively prevented powder from entering the pipe. The maximum powder accumulation height was 10-12 m. Peak gas drainage flow rates for wells 1024-2 and 1024-3 were 32.13 m^3/min and 22.45 m^3/min, respectively, averaging 27.29 m^3/min. The durations with gas flow exceeding 10 m^3/min were 50 days and 41 days, averaging 45.5 days. Although the performance was somewhat lower than that of wells 1022-14 through 1022-17 (which were flushed when the face was directly beneath the well), this mesh-based method is simpler to implement, has lower cost, and still achieves satisfactory powder control and gas drainage.

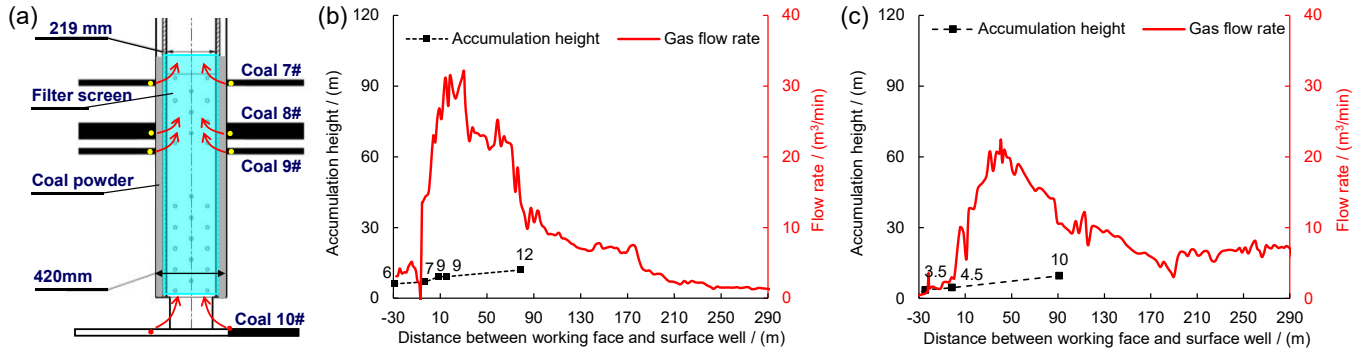


Fig. 12. Test results of coal powder accumulation height and gas drainage flow rate for wells. (a) schematic diagram of

metal mesh installation; (b) well 1024-2; (c) well 1024-3.

4. Discussion

Field observations clearly show that coal powder accumulation severely affects gas drainage performance from surface wells in mining-disturbed areas. Coal powder accumulation reached a maximum height of 101 m, extending up to the roof of the No. 8 coal seam. After the working face passes the well, water cannot drain from the well in time, which then hinders gas entry. This not only reduces gas resource recovery but also prevents timely gas drainage from the goaf, posing a safety risk to underground operations. Three methods were tested to mitigate powder-induced blockage: high-pressure gas flushing, installing a standpipe inside the slotted pipe, and installing a metal mesh filter. Field results show that flushing more than 100 m ahead of the face only temporarily removes powder; subsequent accumulation continues. Flushing after the face has passed the well is also ineffective because fractures connecting the well to the goaf allow injected gas to escape. Installing a standpipe helps maintain connectivity between the well and the goaf. However, if too many drain holes are placed in the standpipe, powder still enters through them. If too few drain holes are used, water levels inside the well do not drop in time, again impairing gas drainage. Therefore, standpipes are not recommended. Compared with gas flushing and standpipe installation, the metal mesh method is low-cost, requires less labor, and is easy to install. A 1.0 mm mesh effectively prevents powder ingress while having only a minor effect on gas flow. It is therefore recommended for future surface wells.

5. Conclusions

Laboratory and field tests were conducted to address coal powder ejection and hole blockage in surface gas drainage wells within soft, strong-outburst coal seams at the Luling Coal Mine. The main conclusions are as follows:

(1) Analysis of coal powder accumulation heights identified two main causes of blockage. First, the adjacent coal seams are soft and prone to pulverization under advanced stress concentration. Second, these seams have high gas pressure and high gas content. After mining-induced pressure relief, gas rapidly desorbs from the adsorbed state to the free state, providing strong pneumatic force for powder ejection.

(2) High-pressure gas flushing was tested in surface wells at the 1022 working face. The best results were obtained when flushing was performed precisely when the working face was beneath the well. Flushing more than 100 m ahead of the face provided only temporary relief, as powder continued to accumulate afterward.

(3) Installing a standpipe inside the slotted pipe was tried as a blockage control method. Field results show that powder still entered the standpipe through drain holes, impairing gas drainage. This method is not recommended.

(4) A metal mesh filter installed outside the slotted pipe was proposed. A laboratory test device was developed to evaluate powder accumulation under different mesh sizes and grouting pressures. Results show that the mesh effectively blocks powder ingress but also reduces gas flow capacity. Considering both powder control and gas drainage performance, a 1.0 mm mesh is recommended. In subsequent field applications at the 1024 working face, wells 1024-2 and 1024-3 fitted with a 1.0 mm mesh achieved good blockage control and satisfactory gas drainage.

Data availability

Yes, availability of Data and Materials. The datasets used and/or analyzed during the current study are available from the corresponding author on reasonable request.

References

[1] Cheng H, Li C (2022) Fault Prevention Structure Design and Application of Ground Gas Drainage Well Tube in Coal Mining Area. Coal

Technol 41:109-111. https://doi.org/10.13301/j.cnki.ct.2022.04.026
[2] Cui J, Li P, Ma D et al (2016) Experiment study on migration law of pulverized coal in borehole of coalbed methane horizontal well. Coal Sci Technol 44:74-79. https://doi.org/10.13199/j.cnki.cst.2016.05.015
[3] Du J, Liu L, Cui J et al (2018) Static settlement of different types of pulverized coal in CBM wells. J China Coal Soc 43:203-209. https://doi.org/10.13225/j.cnki.jccs.2017.1387
[4] Han G, Ling K, Wu H, Gao F, Zhu F, Zhang M (2016) An experimental study of coal-fines migration in Coalbed-methane production wells. J Nat Gas Sci Eng 26:1542-1548. https://doi.org/10.1016/j.jngse.2015.06.012
[5] Hu QT, Sun HT (2014) Graded optimization design method on surface gas drainage borehole. J China Coal Soc 39:1907-1913. https://doi.org/10.13225/j.cnki.jccs.2014.8014
[6] Hua X, Qin H, Hao D, Shi B, Lin B, Zhao Z, Zhang M (2025) Research status and prospect of gas extraction in abandoned/closed coal mines in China. Coal Sci Technol 53:15-28. https://doi.org/10.12438/cst.2024-1511
[7] Huang Z, Li G, Yang R, Li G (2022) Review and development trends of coalbed methane exploitation technology in China. J China Coal Soc 47:3212-3238. https://doi.org/10.13225/j.cnki.jccs.SS22.0669
[8] Jackson P, Kershaw S (1996) Reducing long term methane emissions resulting from coal mining. Energy Convers Manage 37:801-806. https://doi.org/10.1016/0140-6701(96)88504-3
[9] Karacan CO (2015) Analysis of gob gas venthole production performances for strata gas control in longwall mining. Int J Rock Mech Min Sci 79:9-18. https://doi.org/10.1016/j.ijrmms.2015.08.001
[10] Karacan CO, Ruiz FA, Cote M, Phipps S (2011) Coal mine methane: A review of capture and utilization practices with benefits to mining safety and to greenhouse gas reduction. Int J Coal Geol 86:121-156. https://doi.org/10.1016/j.coal.2011.02.009
[11] Khademian Z, Ajayi KM, Schatzel SJ, Esterhuizen GS, Kim BH (2022) Rockmass permeability induced by longwall mining under deep cover: potential gas inflow from a sheared gas well. Min Metall Explor 39:1465-1473. https://doi.org/10.1007/s42461-022-00635-8
[12] Li Q, Li T, Cai Y, Liu D, Li L, Ru Z, Yin T (2023) Research progress on hydraulic fracture characteristics and controlling factors of coalbed methane reservoirs. J China Coal Soc 48:4443-4460. https://doi.org/10.13225/j.cnki.jccs.2023.024
[13] Li R, Xiang W, Xu F, Xiao Y, Lyu S, Zhang X, Zhang L, Yang B (2025) Value and development direction of efficient development of coal-measure natural gas in energy transition. Coal Sci Technol 53:60-72. https://doi.org/10.12438/cst.2024-1493
[14] Li W, Shen J, Ma Z, Pan W, Wang Q, Li C (2025) The migration and deposition patterns of coal fines and their initiation mechanisms during the gas-water two-phase flow stage in coalbed methane wells. Int J Coal Sci Technol 12:83. https://doi.org/10.1007/s40789-025-00815-z
[15] Liu Z, Wei Y, Cao D, You Z, Zhang J, Meng T, Wang A, Yuan Y (2025) Impact of drainage parameters on coal fines production in CBM wells: A long-term monitoring study of Liulin Block, Ordos Basin, China. ACS Omega 10:8361-8373. https://doi.org/10.1021/acsomega.4c10270
[16] Ma L, Liu B, Cui Y, Shi Y (2021) Variations and drivers of methane fluxes from double-cropping paddy fields in southern China at Diurnal, seasonal and inter-seasonal timescales. Water 13:2171. https://doi.org/10.3390/w13162171
[17] Meng Z (2024) Study on new pulverized coal dispersant for fracturing of coalbed gas wells. Saf Coal Mines 55:72-77. https://doi.org/10.13347/j.cnki.mkaq.20221502
[18] Mu T, Ma D, Chen Y et al (2020) Start-migration law of coal powder with different particle sizes under multi-phase flow conditions in coalbed methane wells. Coal Sci Technol 48:188-196. https://doi.org/10.13199/j.cnki.cst.2020.05.026
[19] Palchik V (2003) Formation of fractured zones in overburden due to longwall mining. Environ Geol 44:28-38. https://doi.org/10.1007/s00254-002-0732-7
[20] Ren B, Yuan L, Sang SX, Guo H, Xue J, Huang H, Li Y, Wu J (2018) Deformation and damage of pressure-relieved gas extraction wells in deep mining under thick surface soil and their prevention: With Guqiao of Huainan Mine as an example. Coal Geol Explor 46:159-166. https://doi.org/10.3969/j.issn.1001-1986.2018.05.025
[21] Ren J, Zhang Z, Xing L et al (2025) Output characteristics and control mechanism of coal powder from coalbed methane wells in Shizhuang Block in the south of Qinshui Basin. Saf Coal Mines 56:67-74. https://doi.org/10.13347/j.cnki.mkaq.20231735

[22] Sun HT, Liu DY, Liang YP, Li RF (2009) Key rock strata effecting analysis on surface borehole shear deformation fracture. J Chongqing Univ 32(5):550-555.
[23] Sun HT, Zheng YR, Hu QT, Lin FJ (2011) Surface borehole casing coupling deformation mechanism. J China Coal Soc 36:823-829. https://doi.org/10.13225/j.cnki.jccs.2011.05.028
[24] Wei Y, Li C, Cao D et al (2017) Experiment on screening dispersants of pulverized coal with different sizes in CBM well-washing technology. J China Coal Soc 42:2908-2913. https://doi.org/10.13225/j.cnki.jccs.2017.0322
[25] Wei Y, Xie T, Yang Y, Wei J, Wang Y, Meng T, Zhang J (2022) Impact Factors of Coal Fines Producing from CBM Wells in Liulin Block. Coal Geol China 34:1-5. https://doi.org/10.3969/j.issn.1674-1803.2022.05.01
[26] Xiao L, Chen J (2022) Experimental study on heat transfer caused by feed gas concentration fluctuation in low concentration CBM utilization unit. Heat Mass Transfer 58:355-363. https://doi.org/10.1007/s00231-021-03114-w
[27] Xu X, Chi M, Meng X, Deng J, Liu J, Han G, Lai S (2025) Research on the Settling and Critical Carrying Velocity of Coal Fine in CBM Wells. Processes 13:2289. https://doi.org/10.3390/pr13072289
[28] Yuan L, Guo H, Li P, Liang YP, Liao BC (2013) Theory and technology of goaf gas drainage with large-diameter surface boreholes. J China Coal Soc 38:1-8. https://doi.org/10.13225/j.cnki.jccs.2013.01.015
[29] Zhang DY, Zhu J, Zhao XL, Gao X, Geng M, Chen G, Jiao J, Liu ST (2018) Dynamic assessment of coalbed methane resources and availability in China. J China Coal Soc 43:1598-1604. https://doi.org/10.13225/j.cnki.jccs.2018.4035
[30] Zhang J, Wang Y, Yao N et al (2020) Analysis of coal particles passing screen pipe and test of gas drainage effect in underground coal mine. J China Coal Soc 45:2500-2506. https://doi.org/10.13225/j.cnki.jccs.DZ20.0675
[31] Zhang X, Hu S, You Z, Feng G, Zhao R (2025) Characteristics of coal fine deposition and migration in coalbed methane wells during gas production stage. Phys Fluids 37(4):043321. https://doi.org/10.1063/5.0260989
[32] Zhao X, Liu S, Sang S, Pan Z, Zhao W, Yang Y, Hu Q, Yang Y (2016) Characteristics and generation mechanisms of coal fines in coalbed methane wells in the southern Qinshui Basin, China. J Nat Gas Sci Eng 34:849-863. https://doi.org/10.1016/j.jngse.2016.07.063
[33] Zheng S, Wang L, Chen D, Liu Y, Jiang C (2024) Main control factors of coalbed methane occurrence differences in adjacent coal seams-a case study of Luling coal mine, Huaibei Coalfield, China. Nat Hazards 120:11183-11207. https://doi.org/10.1007/s11069-024-06636-8

Acknowledgments

We would like to thank Wangjun Liu and Chao Ren for their support with data collection.

Author Contributions

W. Qin, Y. Deng, G. Hu and J. Xu conceived and designed the study, H. Duan, W. Ji and L. Che collected the data. All authors contributed to manuscript preparation and approved the final version.

Funding

Open access funding provided by the National Natural Science Foundation of China [Grant No. 52174212, U22A20169].

Declarations

Competing interests

The authors declare that they have no competing interests.

Additional information

Supplementary Information The online version contains supplementary material available at ********.